Regulating Energy Transfer in the ATP Sulfurylase−GTPase System†

Changxian Liu, Ruixiu Wang, Olga Varlamova, and Thomas S. Leyh*

Department of Biochemistry, Albert Einstein College of Medicine, 1300 Morris Park Avenue, Bronx, New York 10461

Received August 12, 1997; Revised Manuscript Received January 6, 1998

ABSTRACT: ATP sulfurylase, isolated from *Escherichia coli K*-12, is a GTPase−target complex that catalyzes and links the energetics of GTP hydrolysis to the synthesis of activated sulfate (APS). When the GTP concentration is saturating and held fixed with a regenerating system, the APS reaction reaches a steady state in which its mass ratio is shifted (5.4×10^6)-fold toward the product by the hydrolysis of GTP. If GTP is not regenerated, the shift toward the product is transient, producing a pulse-shaped progress curve. The mechanistic basis of this transience is the subject of this paper. The product transient is caused by the binding of GDP to the enzyme which establishes a catalytic pathway that allows the chemical potential that had been transferred to the APS reaction to "leak" into the chemical milieu. The system leaks because the E·GDP complex catalyzes the uncoupled APS reaction. The addition of phosphate to the leaky GDP·E·APS·PP_i complex converts it into the central P_i·GDP·E·APS·PP_i complex which catalyzes the energy-transfer reaction. Thus, P_i binding directs the system through the coupled mechanism, "plugging" the leak. GMPPNP, which also causes a leak, is used to demonstrate that the mass ratio of the APS reaction can be "tuned" by adjusting flux through the coupled and uncoupled pathways. This energy-coupling mechanism provides a means for controlling the quantity of chemical potential transferred to the APS reaction. This versatile linkage might well be used to the cell's advantage to avoid the toxicity associated with an excess of activated sulfate.

The metabolic assimilation of sulfate requires that it be chemically activated. Activation overcomes the poor reactivity of sulfate and is accomplished by transferring the adenylyl moiety of ATP from PP_i to SO_4 (reaction 1) (*1*). The adenosine 5′-phosphosulfate (APS) formed in this reaction contains the mixed phosphoric−sulfuric acid anhydride bond that is the hallmark of activated sulfate. $\Delta G^{\circ\prime}$ for the hydrolysis of this bond (−19 kcal/mol (*2*)) is considerably higher than that for the α,β-bond of ATP (−10.7 kcal/mol) which is cleaved in the transfer (*3*). Consequently, the formation of APS and PP_i is extremely unfavorable; the equilibrium constant for reaction 1 is 1.1×10^{-8} at pH 8.0 (*4*). Pyrophosphate hydrolysis could energetically draw reaction 1 forward; however, the high cellular concentration of PP_i in *Escherichia coli* suggests that this reaction is far from equilibrium and therefore might not substantially effect APS synthesis in the cell (*4*). To overcome the unfavorable energetics of APS formation, the cell has linked the chemical potential from the hydrolysis of the β,γ-bond of GTP (reaction 2) to the synthesis of APS in a conformationally coupled reaction that is catalyzed by the enzyme ATP sulfurylase (*4*).

$$ATP + SO_4 \rightleftharpoons APS + PP_i \quad (1)$$

$$GTP + H_2O \rightleftharpoons GDP + P_i + H^+ \quad (2)$$

ATP sulfurylase (ATP:sulfate adenylyltransferase, EC 2.7.7.4) isolated from *E. coli K*-12 is a 390 kDa tetramer of heterodimers (*5*). The subunits of the dimer are CysN (53 kDa), the GTPase subunit, and CysD (23 kDa) which is believed to catalyze APS synthesis (*6*). The mechanism linking these reactions has been studied in some detail (*7*). ATP and GTP bind randomly to the enzyme; GTP hydrolysis precedes, or occurs concomitantly with scission of the α,β-bond of ATP. The α,β-bond scission either precedes or is simultaneous with nucleophilic attack of sulfate, which produces APS. It is the concerted breaking of the β,γ- and α,β-bonds that links the energetics of these two reactions (*4*).

In many bacteria, including *E. coli*, the activation of sulfate is an essential step in the overall eight-electron reduction of sulfate to sulfide, which is incorporated into reduced sulfur metabolites (*8*). Certain anaerobic microorganisms use the reduction of sulfate, rather than oxygen, as an electron sink to drive ATP synthesis (*9*). Mammals use phosphorylated APS or PAPS (3′-phosphate−5′-adenosine phosphosulfate) as the sole sulfuryl group donor. Sulfuryl transfer, much like phosphoryl transfer, switches "on" or "off" target activity (*10*). The sulfuryl group is typically transferred to protein tyrosyl residues or carbohydrate hydroxyl groups. Sulfatases, which hydrolytically remove the SO_3^- group, act in conjunction with transferases to control metabolite activity. For example, the binding of estrogen to its receptor, which activates the receptor, is controlled by sulfation and/or desulfation (*11*, *12*) as is selectin/lymph cell recognition, which is critical to lymphatic circulation (*13*). Sulfating tyrosine 1680 of factor VIII, a protease in the fibrinogen activation cascade, is essential for its proper binding to vonWillebrandt factor (*14*). If it is not sulfated, severe hemophilia A results. Sulfation and/or desulfation is integral

† Supported by National Institutes of Health Grant GM 54469.

* Author to whom correspondence should be addressed: Department of Biochemistry, Albert Einstein College of Medicine, 1300 Morris Park Ave., Bronx, NY 10461. Telephone: (212) 430-2857. Fax: (212) 892-0703. E-mail: Leyh@aecom.yu.edu.

S0006-2960(97)01989-2 CCC: $15.00
Published on Web 02/24/1998

to the proper functioning of many metabolic processes (*15*−*20*).

Under initial rate conditions (saturating GTP, ATP, and SO_4), the rates of GTP hydrolysis and APS synthesis are identical (*4*), which implies that the coupling efficiency is virtually 100%. If the GTP concentration is held fixed using a regenerating system, the APS reaction achieves a steady state in which the mass ratio is 0.059; this is (5.4×10^6)-fold further toward the product than that predicted for the uncoupled reaction (*4*). In the early stages of a reaction in which GTP is not regenerated, APS synthesis is driven by a near-perfect transfer of chemical potential from the hydrolysis reaction. As GDP and P_i accumulate, the reactions are uncoupled. This uncoupling results in a collapse of the APS reaction back to the non-GTP mediated equilibrium position. The mechanism of the uncoupling is described in this paper as are its implications for regulating chemical potential transfer in this and other systems.

MATERIALS AND METHODS

Materials. ATP, GTP, NAD, NADH, PEP,[1] PP_i, glucose, buffers, and salts were the highest grades available from Sigma. Reagent grade triethylamine (TEA) was from Aldrich. Hexokinase (yeast), glucose-6-phosphate dehydrogenase (*Leuconostoc mesenteroides*), pyruvate kinase (yeast), lactate dehydrogenase (rabbit muscle), and guanosine 5′-(β,γ-imido)triphosphate (GMPPNP) were purchased from Boehringer Mannheim. RNA polymerase holoenzyme was obtained from Epicenter Technologies. The Mono-Q HR 5/5 column was purchased from Pharmacia. Polydeoxycytidylic acid, with an average length of 420 base pairs, was from Sigma. [γ-^{32}P]GTP (6000 Ci/mmol), [α-^{32}P]GTP (3000 Ci/mmol), and [α-^{32}P]ATP (3000 Ci/mmol) were purchased from NEN. [^{35}S]SO_4 (6100 Ci/mmol) was obtained from ICN. The poly(ethyleneimine)cellulose-F thin-layer chromatography (PEI−F TLC) plates were obtained from the E. Merck Co. APS was synthesized as previously described (*21*).

Quenching and Quantitating the Radioactive Reactions. In all cases, the reactions were quenched by the addition of EDTA (100 mM, pH 9.5 with KOH) to a final concentration of 33 mM. The quenched solutions were then heated in a boiling water bath for 1 min, spun to pellet precipitate, and spotted onto 10 cm PEI−F TLC plates. The radiolabeled reactants were separated, using the buffer listed in the protocol descriptions, and quantitated using an AMBIS two-dimensional detector. The thin-layer chromatography buffers were TB (0.75 M Tris, 0.45 M HCl, and 0.5 M LiCl) (*22*), FA (4.0 M formic acid, pH 3.5 with NH_4OH) (*22*), SB (0.74 g of $(NH_4)_2SO_4$, 0.4 g of $(NH_4)HSO_4$, 4 g of Na_2EDTA, and 100 mL of H_2O) (*22*), and LiCl (0.90 M) (*23*).

ATP Sulfurylase. The enzyme was purified according to a published protocol from an *E. coli K*-12 strain containing an expression vector that results in the production of high levels of the *E. coli K*-12 enzyme (*5*). The specific activity of the ATP sulfurylase ranged from 0.32 to 0.38 unit/mg. The inorganic pyrophosphatase activity of the preparation was 0.27 munit/mg.

Purification of GMPPNP. Anion exchange chromatography of the commercially available GMPPNP revealed an ∼12% A_{260} contaminant that was reduced to <3% by purification using a Mono-Q HR 5/5 column with a linear salt gradient from 0.0 to 0.60 M triethylamine bicarbonate (TEA/HCO, pH 7.8) (*24*). GMPPNP eluted at 0.42 M TEA. The solvent was removed by rotary evaporation. Residual TEA was removed by suspending and drying the sample three times in methanol, followed by three times in H_2O. The GMPPNP was then suspended in H_2O and the pH adjusted to 7.0 ± 0.2 with KOH.

Synthesis of [α-^{32}P]GDP. Labeled GDP was synthesized by hydrolyzing [α-^{32}P]GTP to [α-^{32}P]GDP and P_i using ATP sulfurylase. The hydrolysis reaction was stimulated using AMP, an allosteric activator of GTP hydrolysis (*25*). The reaction was carried out with ATP sulfurylase (2.0 μM), $MgCl_2$ (2.0 mM), AMP (1.0 mM), Hepes (22 mM, pH 8.0 with K^+), and 250 μCi [α-^{32}P]GTP (2.1 μCi/μL, SA = 3000 Ci/mmol), with $T = 25 \pm 2$ °C. The reaction was run for 30 min and quenched by boiling, and the mixture was spun to remove precipitate and loaded onto a Mono-Q HR 5/5 column. The nucleotides were eluted with a linear gradient of TEA/HCO at pH 7.8. GDP eluted between 0.60 and 0.75 M TEA and was well separated from the other nucleotides. The fractions containing [α-^{32}P]GDP were pooled and dried by rotary evaporation, suspended and dried twice in methanol, suspended and dried twice in distilled deionized water, and suspended in 10 mM Tricine at pH 7.2 (K^+). The reaction yield was 70%. No [α-^{32}P]GTP (i.e. <0.5%) was detected in the [α-^{32}P]GDP.

Initial Rate Assays for ATP Synthesis. The rate of ATP synthesis was monitored at 340 nM by coupling ATP production to the reduction of NAD^+ using the enzymes hexokinase and glucose-6-phosphate dehydrogenase (*26*). Initial rates, with and without activator, were determined in duplicate at each of the 16 conditions obtained using a 4 × 4 matrix of APS and PP_i. The concentration of each substrate was varied, in even increments in reciprocal space, from $\sim 0.2K_m$ to $5K_m$. The activation studies were performed at a fixed, saturating concentration of activator, GMPPNP ($81K_m$) or GDP ($170K_m$). The activator K_m values were obtained by varying the concentration of activator at saturating APS ($190K_m$ and $87K_m$) and PP_i ($120K_m$ and $44K_m$) for GMPPNP and GDP, respectively. In all cases, the consumption of the limiting substrate was kept to less than 10% of that consumed at the end point of the reaction. The assay solutions contained ATP sulfurylase (3.3 munits/mL), hexokinase (0.6 unit/mL), glucose-6-phosphate dehydrogenase (1.8 units/mL), NAD^+ (0.22 mM), $MgCl_2$ ($[PP_i] + 1.0$ mM), and Hepes (50 mM, pH 8.0 with K^+). The kinetic constants of the coupling enzymes were determined in the buffer used in the rate studies, 50 mM Hepes at pH 8.0 with K^+. The kinetic data were fit using the weighted least-squares programs *hypero* and *sequeno* developed by Cleland (*27*).

RNA Polymerase Coupled Assay for GTP Synthesis. The [α-^{32}P]GTP synthesized from [α-^{32}P]GDP and P_i by ATP sulfurylase was converted to poly(G) using the RNA polymerase holoenzyme. At $t = 0$, the reaction conditions were as follows: ATP sulfurylase (0.37 μM), RNA polymerase

[1] Abbreviations: EDTA, ethylenediamine-*N*,*N*,*N*′,*N*′-tetraacetic acid; Hepes, 4-(2-hydroxyethyl)-1-piperazineethanesulfonic acid; PEI−F, poly(ethyleneimine)−fluorescamine; PEP, phosphoenolpyruvate; SA, specific activity; TLC, thin-layer chromatography; Tricine, tris(hydroxymethyl)methylglycine; Tris, tris(hydroxymethyl)aminomethane; unit, micromoles of substrate converted to product per minute at V_{max}.

(0.0031 unit/mL), APS and PP_i (each at 1.0 mM), [α-^{32}P]-GDP (10 μM (18.5K_m), SA = 10−20 nCi/μL), P_i (10, 12, 25, or 50 mM), poly(dC) (50 ng/μL, 69 μM dC residues), $MgCl_2$ ([total nucleotide] + 1.0 mM), and Hepes (50 mM, pH 8.0 with K^+), with T = 25 ± 2 °C. Since the GTP synthesis reaction produces ATP, it was important that the coupling enzyme have a much higher affinity for GTP than ATP. The nucleotide selectivity of RNA polymerase, dictated predominantly by the energetics of correct Waston−Crick base pairing with the template, is ∼10000/1 (*28*−*30*). The energetics of RNA synthesis are very favorable (ca. −2.5 kcal mol^{-1} base added^{-1}) (*31*, *32*).

Controls were performed to evaluate whether the GTP and/or poly(G) synthesis reactions were influenced by the reactants of the complementary reaction. Poly(G) synthesis was not measurably influenced by APS, and GTP synthesis was not effected by poly(C) or RNA polymerase at the concentrations used in the kinetic studies; however, the kinetics and end point of the poly(G) synthesis were influenced by P_i at 50 mM (the highest concentration used in our kinetics studies) and/or PP_i at 1.0 mM. Nevertheless, at 50 mM P_i and 1.0 mM PP_i, ∼10−15% of the GDP was converted to poly(G), and the rate of poly(G) synthesis was sufficiently fast that GTP could not be detected during the reactions. The GTP levels in these reactions were assessed by quantitating radioactive counts at the GTP chromatographic position in two-dimensional PEI−F TLC (first dimension, FA buffer; second dimension, SB buffer; 10 × 10 cm plate). This chromatographic system provided excellent separation of GTP from GDP and background contamination. In all cases, the poly(G) synthesized from [α-^{32}P]-GDP (the concentration-limiting reactant) was <10% of that formed at the end point of the reaction. Duplicate velocities, from separate reactions, were obtained from least-squares fits to five-point time courses. The reactions were quenched, and reactants were separated using FA buffer and quantitated as described above.

RESULTS AND DISCUSSION

A Pulse of Product. A typical progress curve for APS synthesis is represented by the early, or first, pulse shown in Figure 1. The reaction mixture contained GTP but did not contain a GTP-regenerating system. The mass ratio of the APS reaction at the apex of this peak is 1000-fold further toward the product than that predicted in the absence of GTP. At 41 min, indicated by the arrow, a small volume of PEP was added to a final concentration of 300 μM (1.2 times the guanine nucleotide concentration). The system responded to this addition with the second pulse of the product shown in Figure 1. Thus, converting the GDP produced during the first pulse back into GTP (that is, restoring the chemical driving force) is sufficient to cause the transient shift in the mass ratio of the APS reaction.

Superposition of the progress curves for GTP hydrolysis and APS synthesis is shown in Figure 2. The GTP concentration, nearly saturating at t = 0 (79K_m), decreases throughout the pulse to nearly zero. If these reactions were perfectly coupled, their progress curves would plateau as the reactions achieved the equilibrium defined by the sum of the Gibbs potentials for the individual reactions. The chemical potential of the reactions would be conserved,

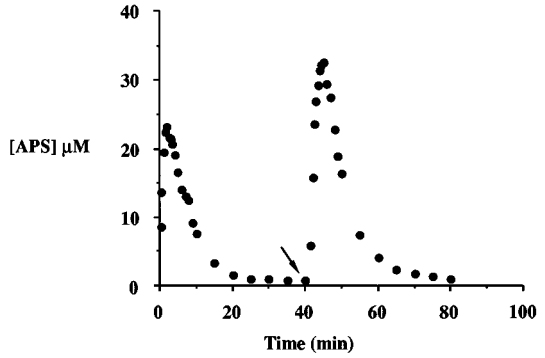

FIGURE 1: Transient synthesis of product. Two pulse-shaped progress curves for APS synthesis are shown. At t = 0, the experimental conditions were as follows: ATP sulfurylase (4.0 μM), ATP (0.50 mM), GTP (0.25 mM), [^{35}S]SO_4 (0.10 mM, SA = 20−30 nCi/μL), $MgCl_2$ (1.75 mM), pyruvate kinase (6.0 munits/μL), and Hepes (50 mM, pH 8.0/K^+), T = 25 ± 2 °C. At 41 min (indicated by the arrow), 0.80 μL of 100 mM PEP was added to 276 μL of the reaction mixture (0.29 mM final concentration). This addition regenerates the hydrolyzed GTP. The reactions were quenched, and reactants were separated, using LiCl buffer, and quantitated as described in Materials and Methods. Each point is the average of two determinations.

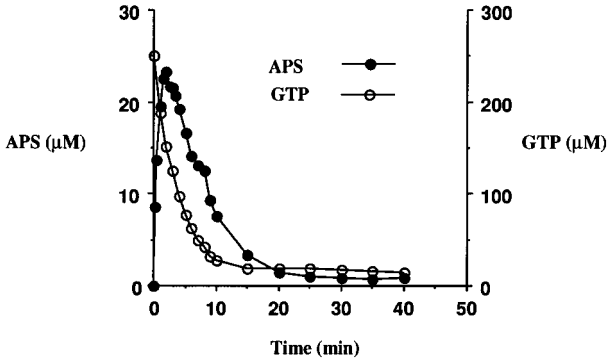

FIGURE 2: Superposition of the progress curves for GTP hydrolysis and APS synthesis. The APS data is the same as that for the earlier pulse shown in Figure 1. The GTP reactions were identical to those describe in the Figure 1 legend except that they contained [α-^{32}P]-GTP (SA = 20−30 nCi/μL) rather than [^{35}S]SO_4. GA buffer was used to separate [α-^{32}P]GTP and [α-^{32}P]GDP (Materials and Methods). Each point is the average of two determinations.

despite changes in their mass ratios, because the potential lost by one reaction is transferred to the other. If, however, there were an uncoupled catalytic path for even one of the reactions, the chemical potential would leak out of the coupled system with the result being that each reaction would eventually reach its non-linked equilibrium position. This leak model is consistent with the data shown in Figures 1 and 2. The pulse of product suggests that the potential associated with GTP hydrolysis, initially used to drive the synthesis of APS and PP_i, is eventually drained from the system, resulting in the collapse of the APS reaction back to its non-linked equilibrium position.

The pulse can be explained in two ways. The first of these is that the APS reactants are interconverting throughout the pulse. In this case, the observed changes in mass ratio are caused by changes in the relative rates of the forward and reverse reactions, which appear to depend on the position of the GTP hydrolysis reaction. The second interpretation is that the addition and consumption of GTP generates a bolus of APS which subsequently hydrolyzes, producing AMP and SO_4. This latter possibility, unlikely at the pH of

this experiment (*33*), was ruled out by performing experiments identical to those shown in Figure 2 except that the ATP was radiolabeled ([α-^{32}P]ATP). AMP was not detected (data not shown).

Rate Changes during the Pulse. The fact that AMP is not formed in these reactions confirms that the transient is caused by changes in the rate of synthesis and consumption of product during the pulse. These net rates are the composite of the rates of all paths (linked and unlinked) between substrate and product and appear to be sensitive functions of the position of the GTP hydrolysis reaction. We were interested in knowing how the rates of the forward and reverse reactions change throughout the pulse and in how these changes are linked to GTP hydrolysis. To determine how the rates change, a small volume (5% of the reaction volume) of radiolabeled substrate or product was added to the reaction at various time points throughout the pulse. The rate of conversion of the labeled compound to product was measured over the 10 s interval following its addition. During this short interval, the concentrations of substrate and product do not change significantly; hence, this experiment measures the rate at which isotope is transferred between static reactant pools. The reactions were allowed to proceed to <10% of their end points to prevent significant back reaction during the measurements.

The changes in the instantaneous rates of the forward and reverse reactions during the pulse are shown in panels A−C of Figure 3. The rate of APS synthesis descends, as GTP is consumed, from a maximum of 1.0 μM s^{-1}, at $t = 0$, to 0.06 μM s^{-1} in the descending tail of the pulse (panel A). The rate at which ATP and SO_4 are produced from APS and PP_i increases from $t = 0$ to the apex of the pulse, at which point the forward and reverse reaction rates are equal. The rate of ATP synthesis then decreases as the GTP hydrolysis reaction approaches completion and the APS reaction re-establishes its non-linked equilibrium position (panel B). The rate of GTP hydrolysis is maximum and equal to that of APS synthesis at $t = 0$. Like the APS synthesis reaction, the rate of GTP hydrolysis decreases throughout the pulse (panel C). GTP synthesis was not detected during the pulse. The lower limit of detection of this [^{32}P]P_i experiment is approximately 0.5 nM/s.

The lack of detectable GTP synthesis during the pulse means that the synthesis of ATP and SO_4 occurs almost exclusively through an uncoupled catalytic pathway, or leak, and that the flux through the leak is equivalent to the velocity of the ATP synthesis reaction, accelerating to the apex of the pulse and decelerating thereafter (panel B). Due to the very unfavorable energetics for APS formation in the absence of GTP, APS is not detected under the experimental conditions associated with Figure 3, without the addition of GTP. Thus, panel A represents the acceleration versus deceleration profile of the APS synthesis reaction through the coupled catalytic pathway.

Nonproductive Complexes Erode Coupling Efficiency. At saturating concentrations of ATP, SO_4, and GTP, the initial rates of GTP hydrolysis and APS synthesis are identical (*4*). This well-defined 1:1 stoichiometry indicates that the coupling efficiency of the E·ATP·SO_4·GTP complex approaches 100%. GTP hydrolysis is activated to varying degrees by the reactants of the APS reaction. The allosteric interactions linking the energetics of GTP hydrolysis to the

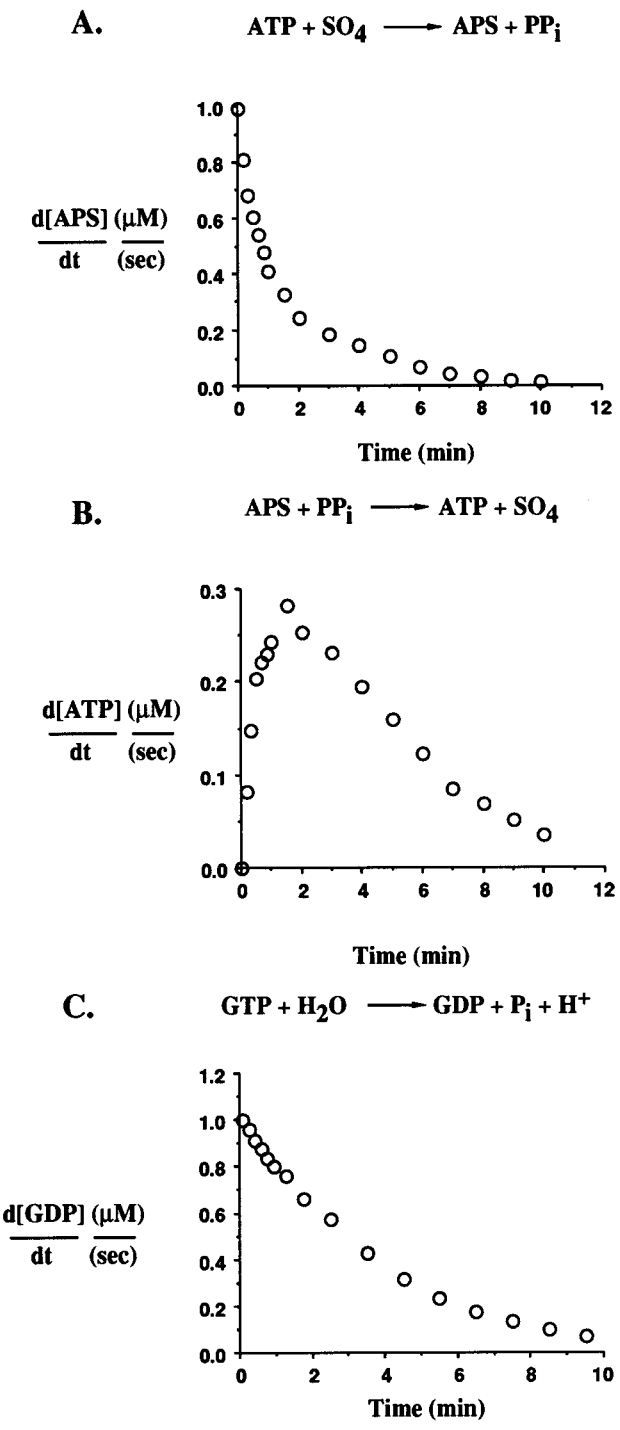

FIGURE 3: Initial rates of the forward and reverse directions of the APS synthesis and GTP hydrolysis reactions at various time points throughout the pulse. (A) ATP + SO_4 → APS + PP_i. (B) APS + PP_i → ATP + SO_4. (C) GTP + H_2O → GDP + P_i + H^+. GTP synthesis could not be detected during the pulse. The velocities were determined by adding 1.0 μL of radiolabeled compound to 20 μL of reaction mixture, quenching the reactions 10 s later, and quantitating product. The extent of isotope exchange was always <10% of its end point. In each case, the reaction conditions were as follows: ATP sulfurylase (2.0 μM), GTP (0.25 mM), ATP (0.50 mM), SO_4 (0.10 mM), $MgCl_2$ (1.75 mM), and Hepes (50 mM, pH 8.0/K^+), $T = 25 \pm 2$ °C. The radiochemicals used in these experiments were (A) [^{35}S]SO_4, (B) [^{35}S]APS, and (C) [γ-^{32}P]GTP. The specific activities of the radionuclides were 20−30 nCi/μL. The reactions were quenched, and reactants were separated, using LiCl buffer, and quantitated as described in Materials and Methods. Each data point is the average of two determinations.

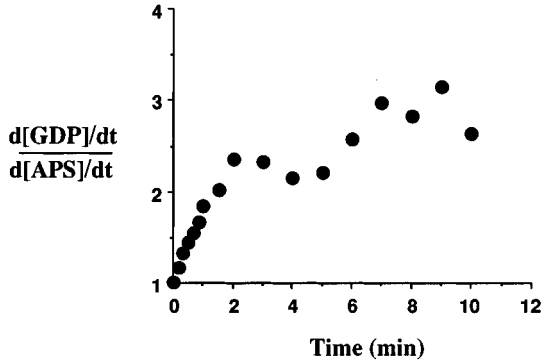

FIGURE 4: Erosion of coupling efficiency. The ratio of the initial rates of GTP hydrolysis to APS synthesis were calculated from the data shown in panels A and C of Figure 3.

Table 1: Activation of APS Synthesis

activator substrate	K_i (μM)	K_m (μM)	k_{cat} (s^{-1})
APS	156 (8)	49 (1.5)	0.76 (0.067)
PP_i	164 (9)	51 (1.5)	
APS	47 (4.3)	11 (0.6)	
PP_i	35 (3.2)	8.0 (0.5)	1.3 (0.022)
GDP		0.51 (0.23)	
APS	15 (1.4)	7.8 (0.43)	
PP_i	20 (2.0)	10 (0.48)	1.3 (0.019)
GMPPNP		1.5 (0.20)	

formation of binary and ternary complexes at the APS-forming active site have been studied (*25*, *34*). The rate of GTP hydrolysis at any instant in the pulse is determined by the ensemble of complexes present at that moment. Over time, the ensemble changes. As product forms, it competes with substrate for the enzyme, resulting in nonproductive or futile hydrolysis of GTP which erodes the coupling efficiency of the system. The change in coupling efficiency of these reactions during the pulse is revealed by taking the ratio of the initial rates of GTP hydrolysis to APS synthesis, obtained from the data shown in panels C and A of Figure 3. The result of this operation is shown in Figure 4. The coupling efficiency, ~100% in the initial portion of the curve, decreases as the reactions proceed with GTP hydrolysis exceeding ATP synthesis in the tail of the pulse by ~3.

The Binding of GDP Causes a Thermodynamic Leak. The erosion of coupling efficiency and acceleration of the uncoupled ATP synthesis reaction with the concomitant production of GDP and P_i suggest that one, or both, of the hydrolysis products causes the reactions to uncouple. GDP was tested as an uncoupler in an initial rate study of the effects of GDP on the synthesis of ATP and SO_4 (see Materials and Methods for experimental details). The results were that GDP slightly activates ATP synthesis compared to control reactions without GDP (Table 1). The affinities of APS and PP_i were increased 2.9- and 1.9-fold, respectively; k_{cat} is increased 1.7-fold. The K_m of GDP for the E·APS·PP_i complex (0.54 μM) is 12-fold lower than that for GTP in the forward reaction (6.3 μM) (*25*).

The fact that the E·GDP complex catalyzes ATP synthesis means that the binding of GDP provides a catalytic pathway, or leak, through which ATP synthesis can occur without being coupled to GTP synthesis. GDP competes with GTP for the guanine nucleotide binding site of ATP sulfurylase (*4*). The increasing [GDP]/[GTP] ratio throughout the pulse

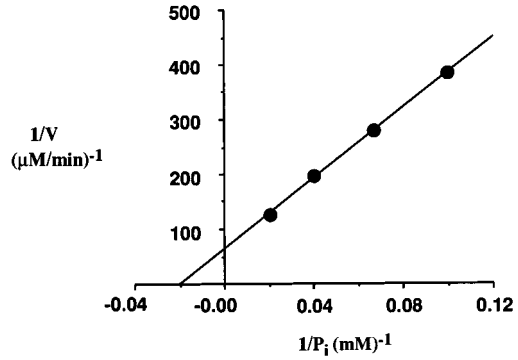

FIGURE 5: Initial rate of GTP synthesis versus phosphate concentration. The synthesis of [α-^{32}P]GTP, from [α-^{32}P]GDP and P_i, was coupled to the synthesis of poly(G) by RNA polymerase. GTP synthesis required APS and PP_i (see the text). The reaction solutions contained ATP sulfurylase (0.37 μM), RNA polymerase (0.04 unit/mL), APS (1.0 mM), PP_i (1.0 mM), GDP (10 μM), P_i (10, 12, 15, or 50 mM), poly(dC) (50 ng/μL, 69 μM dC residues), $MgCl_2$ ([total nucleotide] + 1.0 mM), and Hepes (50 mM, pH 8.0/K^+), $T = 25 \pm 2$ °C. Each point is the average of at least two determinations. The reactions were quenched and the reactants separated (FA buffer) and quantitated as described in Materials and Methods.

alters the ratio of enzyme forms that catalyze the coupled and uncoupled reactions. This ratio of enzyme forms determines the flux through the coupled and uncoupled pathways and, ultimately, the mass ratio of the APS reaction.

Coupled Synthesis of GTP and the K_m of Phosphate. At concentrations of phosphate greater than 5 mM, the synthesis of GTP by ATP sulfurylase can be detected in a reaction that requires APS and PP_i. To evaluate the kinetic constants associated with GTP hydrolysis, the initial rate of GTP synthesis was studied as a function of phosphate concentration at near-saturating concentrations of APS ($58K_m$), PP_i ($37K_m$), and [α-^{32}P]GDP ($18K_m$). Due to the fact that the GTP synthesized by ATP sulfurylase is eventually hydrolyzed through uncoupled pathways, it was necessary to quickly convert the GTP as it is synthesized to a compound that is stable toward hydrolysis. This requires a coupling enzyme that has a high affinity for GTP, little or no affinity for ATP (which is produced in the reaction), and favorable overall energetics. These criteria were well satisfied by the RNA polymerase holoenzyme, using a poly(C) template (see Materials and Methods). Under the conditions described in the Figure 5 legend, the RNA polymerase activity was 1200 times greater than the V_{max} for the synthesis of GTP by ATP sulfurylase. Thus, the steady state level of GTP was very low; GTP could not be detected in these assays (<50 nM). The synthesis of labeled poly(G) required the presence of both APS and PP_i; thus, the synthesis of GTP is coupled to the formation of ATP and SO_4.

The results of the GTP synthesis initial rate study are shown in Figure 5. The K_m of phosphate for the central complex is quite high (44 ± 13 mM), and V_{max} is extremely low (0.015 ± 0.0025 μM min^{-1}). This very low affinity of phosphate explains why GTP hydrolysis and APS synthesis are uncoupled by GDP during the pulse. The P_i concentration, which reaches a maximum of 0.50 mM during the pulse, is simply too low to prevent the uncoupling.

Phosphate Plugs the Leak. The only complexes capable of catalyzing the coupled chemistries are the central com-

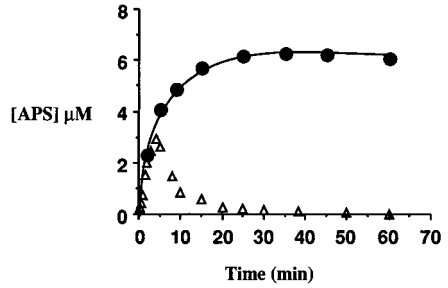

FIGURE 6: Effect of a high concentration of phosphate (0.20 M) on the progress curve for APS synthesis. The conditions of this experiment were as follows: ATP sulfurylase (1.0 μM), ATP (0.20 mM), [^{35}S]SO_4 (0.20 mM, SA = 20 μCi/μL), GTP (0.10 mM), P_i [0.20 M (●) or 0.0 (△)], and Hepes (50 mM, pH 8.0/K^+), T = 25 ± 2 °C. Each point was determined in duplicate. The reactions were quenched, and the radiolabeled reactants were separated, using a 0.90 M LiCl mobile phase, and quantitated as described in Materials and Methods.

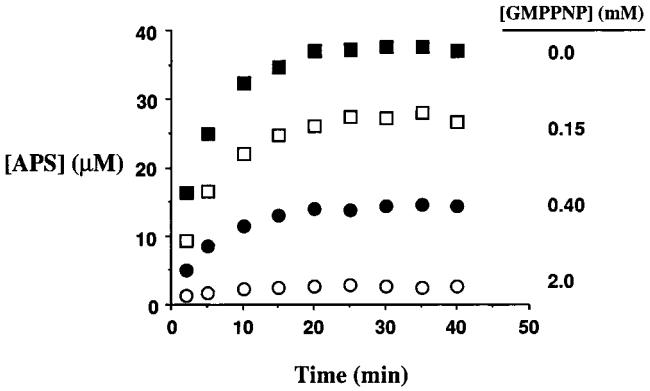

FIGURE 7: GMPPNP influences the mass ratio of the APS reaction. The GMPPNP concentration fixes the flux through the coupled and uncoupled pathways, thereby regulating the steady state mass ratio of the APS reaction. The reaction conditions were as follows: ATP sulfurylase (0.50 μM), ATP (0.20 mM), [^{35}S]SO_4 (0.20 mM, SA = 20 μCi/μL), GTP (1.0 mM), GMPPNP [2.0 mM (○), 0.40 mM (●), 0.15 mM (□), and 0.0 (■)], $MgCl_2$ ([total nucleotide] + 1.0 mM), pyruvate kinase (8.0 units/mL), PEP (5.0 mM), and Hepes (50 mM, pH 8.0/K^+), T = 25 ± 2 °C. The reactions were quenched, and reactants were separated, using LiCl buffer, and quantitated as described in Materials and Methods. Each point is the average of two determinations.

plexes, GTP·E·ATP·SO_4 and GDP·P_i·E·APS·PP_i. If the concentration of phosphate were sufficiently high to drive essentially all of the leaky, GDP·E·APS·PP_i complex into the product central complex, the leak would be slow, and one would observe the trailing edge of the pulse only over long periods of time. The data in Figure 6 demonstrate that this is indeed the case. At a high phosphate concentration (0.20 M) and without a GTP-regenerating system, the progress curve for APS synthesis reaches a long-lived plateau. The control reaction mixture, containing no added phosphate, gave a typical product transient. Thus, phosphate acts as a molecular "plug" in that it prevents leaking and enforces coupling when it binds to and converts the leaky GDP complex into the central product complex. The mass ratio for the APS reaction in the plateau of the progress curve obtained at high phosphate concentrations is 1.1×10^{-3}. This (1×10^5)-fold shift toward product corresponds to a transfer of −6.8 kcal/mol to the APS reaction.

These studies have some bearing on the somewhat ill-defined issue of the functional properties of ternary GTPase·GDP·P_i complexes. The potential prevalence of these species in the cell becomes apparent when one considers that the in vivo concentration of phosphate [e.g., 4−42 mM in skeletal muscle under various exercise conditions (*35*)] is comparable to the estimated affinity of phosphate for the binary RAS·GDP complex ($K_d \sim 12$ mM) (*36*). Thus, a significant fraction of a given GTPase might well be in the ternary complex in the cell. While the importance of phosphate binding in GTPase function has been discussed, the literature appears to contain little or no direct experimentation on this point. Our finding, that the ternary complex of the ATP sulfurylase−GTPase is functionally distinct from either the GTP or GDP binary complexes, suggests that other GTPase ternary complexes may also have unique functional and/or regulatory properties.

A Constant Leak Produces a Steady State. The concentrations of GTP, GDP, and P_i have been determined in asynchronous, logarithmic cultures of *E. coli*; they are 920 μM, 130 μM, and 10 mM, respectively (*35*−*37*). We do not yet know how the cellular concentrations of these metabolites vary as a function of cell cycle or nutrient challenge or within unique microenvironments of the cell. If, as is generally assumed, these compounds reach a steady state, one expects that the flux through the coupled and uncoupled pathways would be constant, resulting in a steady state for the APS chemistry.

GMPPNP, like GDP, competitively inhibits the binding of GTP and slightly activates the uncoupled reaction (see Table 1). By fixing the concentration of GTP, using a regenerating system, and varying the concentration of GMPPNP, one can simulate the effects of varying the GTP/GDP ratio on the APS reaction. The results of such an experiment are shown in Figure 7. The steady state mass ratio of the APS reaction is determined by the concentration of GMPPNP. Thus, regulating flux through the coupled and uncoupled pathways can be used to control the mass ratio of the APS reaction.

A Metabolic Rationale. The question of why the cell might want to regulate linking the energetics of APS synthesis and GTP hydrolysis cannot be answered with certainty due to our incomplete understanding of both the metabolism of this pathway and the in vivo milieu. However, a rationale is provided by the fact that PAPS, or a derivative(s) of it, is a toxic metabolite in *E. coli* and *Salmonella typhimurium*. This toxicity issue has been investigated in genetic studies in which three different protein functions, each acting at the point of PAPS consumption, were mutagenically blocked (*38*−*40*). In each case, the mutant bacteria grew poorly, or not at all, under conditions that induce the enzymes that synthesize PAPS. When subjected to these toxic conditions, cells rapidly acquire second-site mutations that block PAPS synthesis. In one case, second-site mutation was essential for viability (*40*). Controlling the coupling efficiency of ATP sulfurylase, a step prior to PAPS synthesis, would enable the cell to avoid accumulation of the toxin(s) by regulating metabolic flux through the pathway.

At some point in the evolution of *E. coli*, it became advantageous for the cell to link the synthesis of activated sulfate to a reservoir of chemical potential that could be used to drive this unfavorable chemistry. GTP hydrolysis was selected for this purpose. The potential associated with

hydrolysis, or any energy-donating reaction, is immutable in a given chemical environment. If it is too large, it can drive the linked event too far and disrupt proper metabolic balance. Faced with this situation, the cell must find a way to titrate the transfer of potential from the reservoir into the linked reaction. One solution to this problem is to evolve a conduit for the transfer of chemical potential whose linking efficiency satisfies the complex metabolic constraints placed on the organism.

CONCLUSIONS

The mass ratio of the APS reaction is determined, in large part, by the efficiency with which this reaction is linked to the energetics of GTP hydrolysis by ATP sulfurylase. The efficiency is determined by the distribution of guanine nucleotide-bound forms of the enzyme. GDP inhibits the coupled reaction, by preventing the binding of GTP, while allowing the uncoupled chemistry to occur. Thus, GDP binding causes the system to leak. The binding of phosphate to the GDP·E·APS·PP_i complex results in a central complex that catalyzes the coupled synthesis of GTP to the synthesis of ATP and SO_4. Phosphate binding plugs the leak by driving the system through the coupled catalytic pathway. This versatile mechanism provides a means of titrating the transfer of chemical potential between two reactions and could be used by the cell to regulate the transfer of chemical energy in metabolism.

REFERENCES

1. De Meio, R. M. (1975) in *Metabolic Pathways* (Greenberg, D. M., Ed.) Vol. VII, pp 287−347, Academic Press, New York.
2. Robbins, P. W., and Lipmann, F. (1958) *J. Biol. Chem. 233*, 686−690.
3. Leyh, T. S., and Suo, Y. (1992) *J. Biol. Chem. 267*, 542−545.
4. Liu, C., Suo, Y., and Leyh, T. S. (1994) *Biochemistry 33*, 7309−7314.
5. Leyh, T. S., Taylor, J. T., and Markham, G. H. (1987) *J. Biol. Chem. 263*, 2409−2416.
6. Leyh, T. S., Vogt, T. F., and Suo, Y. (1992) *J. Biol. Chem. 267*, 10405−10410.
7. Liu, C., Martin, E., and Leyh, T. S. (1994) *Biochemistry 33*, 2042−2047.
8. Siegel, L. M. (1975) in *Metabolic Pathways* (Greenberg, D. M., Ed.) Vol. VII, pp 217−276, Academic Press, New York.
9. Singleton, R. J. (1993) in *The Sulfate Reducing Bacteria: Contemporary Perspectives* (Odom, J. M., and Singleton, R. J., Eds.) pp 1−20, Springer-Verlag, New York.
10. Leyh, T. S. (1993) *Crit. Rev. Biochem. Mol. Biol. 28*, 515−542.
11. Gorski, J., and Shymala, G. (1968) *J. Biol. Chem. 244*, 1097−1103.
12. Merriam, G. R., MacLusky, N. J., Picard, M. K., and Naftolin, F. (1980) *Steriods 36*, 1−11.
13. Hemmerich, S., Bertozzi, C. R., Leffler, H., and Rosen, S. D. (1994) *Biochemistry 33*, 4820−4829.
14. Leyete, A., van Schijndel, H. B., Niehrs, C., Huttner, W. B., Verbeet, M. P., Mertens, K., and van Mourik, J. A. (1991) *J. Biol. Chem. 266*, 740−746.
15. Falany, C. N., Wheeler, J., Oh, T. S., and Falany, J. N. (1994) *J. Steroid Biochem. Mol. Biol. 48*, 369−375.
16. Roth, J. R., and Rivett, A. J. (1982) *Biochem. Pharmacol. 31*, 3017−3021.
17. Brand, S. J., Andersen, B. N., and Rehfeld, J. F. (1984) *Nature 309*, 456−458.
18. Garay, R. P., Labaune, J. P., Mesangeau, D., Nazaret, C., Imbert, T., and Moinet, G. (1990) *J. Pharmacol. Exp. Ther. 255*, 415−422.
19. Hortin, G. L., Farries, T. C., Graham, J. P., and Atkinson, J. P. (1989) *Proc. Natl. Acad. Sci. U.S.A. 86*, 1338−1342.
20. Ishihara, M., Guo, Y., and Swiedler, S. J. (1993) *Glycobiology 3*, 83−88.
21. Baddiley, J., Buchanan, G. J., and Letters, R. (1957) *J. Chem. Soc.*, 1067−1071.
22. Bochner, B. R., and Ames, B. N. (1982) *J. Biol. Chem. 257*, 9759−9769.
23. Randerath, K., and Randerath, E. (1964) *J. Chromatogr. 16*, 111−125.
24. Porath, J. (1955) *Nature 11*, 478.
25. Wang, R., Liu, C., and Leyh, T. S. (1995) *Biochemistry 34*, 490−495.
26. Lamprecht, W., and Trautschold, I. (1974) *Methods Enzymol. Anal. 4*, 2101−2110.
27. Cleland, W. W. (1979) *Methods Enzymol. 63*, 103−138.
28. Rackwitz, H. R., and Scheit, K. H. (1977) *Eur. J. Biochem. 72*, 191−200.
29. Blank, A., Gallant, J. A., Burgess, R. R., and Loeb, L. A. (1986) *Biochemistry 25*, 5920−5928.
30. von Hipple, P. H., Bear, D. G., Morgan, W. D., and McSwiggen, J. A. (1984) *Annu. Rev. Biochem. 53*, 389−446.
31. Kahn, J. D., and Hearst, J. E. (1989) *J. Mol. Biol. 205*, 291−314.
32. Krakow, J., and Fonk, E. (1969) *J. Biol. Chem. 224*, 5988−5993.
33. Bedford, C. T., Kirby, A. J., Logan, C. J., and Drummond, J. N. (1995) *Bioorg. Med. Chem. 3*, 167−172.
34. Yang, M., and Leyh, T. S. (1997) *Biochemistry 36*, 3270−3277.
35. Wang, R., Liu, C., and Leyh, T. S. (1995) *Biochemistry 34*, 490−495.
36. Neuhard, J., and Nygaard, P. (1987) in *Escherichia Coli and Salmonella Typhimurium Cellular and Molecular Biology* (Neidhardt, F. C., Ed.) pp 445−473, American Society for Microbiology, Washington, DC.
37. Rao, N. N., Roberts, M. F., Torriani, A., and Yashphe, J. (1993) *J. Bacteriol. 175*, 74−79.
38. Gillespie, D., Demerec, M., and Itikawa, H. (1968) *Genetics 59*, 433−442.
39. Newald, A. F., Krishnan, B. R., Brikun, I., Kulakauskas, S., Suziedelis, K., Tomcsanyi, T., Leyh, T. S., and Berg, D. E. (1992) *J. Bacteriol. 174*, 415−425.
40. Russel, M., Model, P., and Holmgren, A. (1990) *J. Bacteriol. 172*, 1923−1929.

BI971989D